Accepted for Publication in ApjL
Preprint typeset using LaTeX style emulateapj v. 11/10/09

TIGHTLY CORRELATED HI AND FUV EMISSION IN THE OUTSKIRTS OF M83

F. Bigiel[1,2], A. Leroy[3,6], M. Seibert[4], F. Walter[2], L. Blitz[1], D. Thilker[5], B. Madore[4]

Accepted for Publication in ApjL

ABSTRACT

We compare sensitive H I data from The H I Nearby Galaxy Survey (THINGS) and deep far UV (FUV) data from GALEX in the outer disk of M83. The FUV and H I maps show a stunning spatial correlation out to almost 4 optical radii (r_{25}), roughly the extent of our maps. This underscores that H I traces the gas reservoir for outer disk star formation and it implies that massive (at least low level) star formation proceeds almost everywhere H I is observed. Whereas the average FUV intensity decreases steadily with increasing radius before leveling off at $\sim 1.7 r_{25}$, the decline in H I surface density is more subtle. Low H I columns ($\lesssim 2\,M_\odot$ pc^{-2}) contribute most of the mass in the outer disk, which is not the case within r_{25}. The time for star formation to consume the available H I, inferred from the ratio of H I to FUV intensity, rises with increasing radius before leveling off at ~ 100 Gyr, i.e., many Hubble times, near $\sim 1.7 r_{25}$. Assuming the relatively short H_2 depletion times observed in the inner parts of galaxies hold in outer disks, the conversion of H I into bound, molecular clouds seems to limit star formation in outer galaxy disks. The long consumption times suggest that most of the extended H I observed in M83 will not be consumed by *in situ* star formation. However, even these low star formation rates are enough to expect moderate chemical enrichment in a closed outer disk.

Subject headings: galaxies: evolution — galaxies: ISM — galaxies: individual (M83) — radio lines: galaxies — stars: formation

1. INTRODUCTION

In this letter we compare wide-field images of atomic hydrogen (H I) and far ultraviolet (FUV) emission, a tracer of recent star formation (SF), in the far outer disk of the nearby spiral galaxy M83. Star formation in the outer disks of galaxies has been the subject of numerous studies, including direct optical observations of massive SF (e.g., Ferguson et al. 1998; Lelièvre & Roy 2000; Cuillandre et al. 2001; de Blok & Walter 2003) and studies of the star-forming interstellar medium (ISM) using CO emission (Braine et al. 2007; Gardan et al. 2007) or dust (Zaritsky 1994; Popescu & Tuffs 2003). With its large field-of-view and excellent sensitivity, the *Galaxy Evolution Explorer* (GALEX) revolutionized this field, revealing widespread, extended SF in the far outer reaches (i.e., far beyond the optical disks) of many galaxies (Thilker et al. 2005, 2007, 2009; Gil de Paz et al. 2005, 2007a; Boissier et al. 2007). At the same time it has long been known that many galaxies host extended H I distributions (e.g., Bosma 1981; Kamphuis & Briggs 1992; Bajaja et al. 1994; Boomsma et al. 2008; Walter et al. 2008) – including M83 (e.g., Huchtmeier & Bohnenstengel 1981).

Mainly due to the lack of matched wide-field and sensitive UV and 21 cm observations, it is still largely unclear how these two extended components – star formation traced by FUV emission and atomic hydrogen – relate to one another. Although the integrated star formation rates (SFRs) in extended UV (XUV) disks represent only a small fraction of the total SFR, the H I-SFR connection at large radii bears on a number of aspects of galaxy structure and evolution, such as the shapes and edges of stellar disks (Pohlen & Trujillo 2006) or chemical enrichment gradients across galaxies (Gil de Paz et al. 2007b). The consumption of outer disk H I by SF affects the availability of this gas for fueling SF in inner galaxy disks, a necessary process for galaxies to sustain SF over cosmological times (e.g., Shlosman, Frank & Begelman 1989; Blitz 1996; Bauermeister et al. 2009). Finally, comparing UV and H I in the extreme (low-density, often low-metallicity) environment of outer galaxy disks can illuminate the limiting conditions for cloud and star formation ("star formation threshold").

In this letter we combine sensitive, large field-of-view H I data from THINGS (The H I Nearby Galaxy Survey, Walter et al. 2008) with extremely deep FUV data from GALEX to study the relationship between H I (the dominant component of the ISM at large radii) and FUV emission in the nearby spiral galaxy M83. Previous, shallower GALEX observations showed that M83 hosts one of the most prominent examples of a XUV disk (Thilker et al. 2005, 2007). This unique data set allows us to trace the distribution of H I and FUV emission across a $\sim 50'$ field-of-view, corresponding to almost 4 optical radii r_{25} (defined as the 25th B-band mag arcsec^{-2} isophote). We use these data to measure the location (§ 3) and amount (§ 4) of FUV emission relative to the H I. In Section § 5 we investigate the distribution of H I surface densities in different radial regimes across M83.

[1] Department of Astronomy, Radio Astronomy Laboratory, University of California, Berkeley, CA 94720, USA; bigiel@astro.berkeley.edu
[2] Max-Planck-Institut für Astronomie, Königstuhl 17, 69117 Heidelberg, Germany
[3] National Radio Astronomy Observatory, 520 Edgemont Road, Charlottesville, VA 22903, USA
[4] Observatories of the Carnegie Institution of Washington, Pasadena, CA 91101, USA
[5] Center for Astrophysical Sciences, Johns-Hopkins University, 3400 North Charles Street, Baltimore, MD 21218, USA
[6] Hubble Fellow

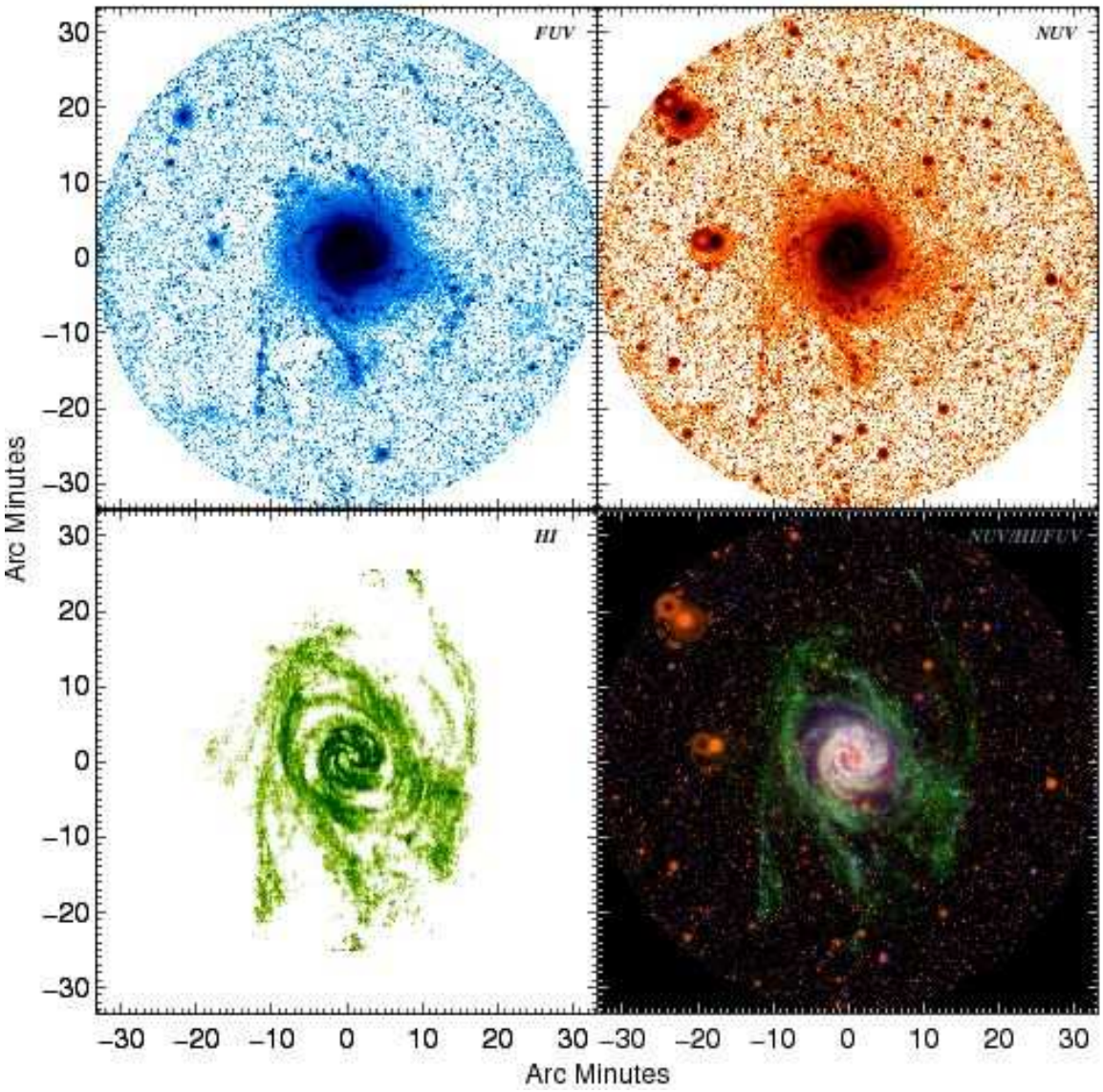

FIG. 1.— GALEX far UV (upper left), near UV (upper right), THINGS HI (lower left) maps of M83 and a combination of smoothed HI, near, and far UV (lower right). The axes show the offset from the field center at R.A. = $13^h37^m1.2^s$ and Dec. = $-29°52'16''$. The exposure time for the UV data is 13.5 ks, which makes it one of the deepest UV integrations on a nearby galaxy to date. The UV maps reveal a rich spiral structure within the star forming disk, a diffuse extended envelope of UV emission and multiple arms, arcs and filaments that reach out to almost 4 optical radii (i.e., roughly the edge of the map). All these structures show a stunning degree of correlation with the HI map, indicating (qualitatively) a tight spatial correlation of atomic hydrogen and UV emission far into the outer disk of M83.

2. DATA & METHODOLOGY

We use H I data from the NRAO[7] VLA obtained as part of THINGS to construct a map of H I 21 cm emission across a $\sim 50'$ field-of-view (Figure 1, lower left panel). This map has been corrected for primary beam attenuation (the VLA primary beam FWHM is $\sim 30'$). To maximize sensitivity for extended emission, we apply the "natural" weighting scheme, which yields a sensitivity (1σ RMS) of ~ 0.8 mJy/beam (or $\sim 0.2\,M_\odot pc^{-2}$) and a resolution of $\sim 13''$. M83 is known to contain a significant amount of its total H I content in the form of diffuse, low column density H I in its outer disk (e.g., Huchtmeier & Bohnenstengel 1981), which our interferometric observations will not pick up by design. Because we are focussing on H I emission associated with (localized) star formation, the potentially missing flux on very large ($\gtrsim 15'$) scales is not a concern in the current study. When quoting H I surface densities we include a factor of 1.36 to account for helium and heavier elements.

The GALEX FUV data are part of our GI program GI3-050. Due to two bright stars near M83, the GALEX observations were carried out in petal pattern mode allowing for the field-of-view to be centered on the galaxy. The GALEX field-of-view is slightly larger than the area covered by the H I map. We thus restrict our analysis to the $\sim 50'$ field covered by both maps. M83 was observed for 9 orbits (~ 13.5 ks) yielding a FUV map about three times as sensitive as the GALEX Nearby Galaxy Survey M83 map (Gil de Paz et al. 2007a). We use a gaussian

[7] The National Radio Astronomy Observatory is a facility of the National Science Foundation operated under cooperative agreement by Associated Universities, Inc.

kernel to degrade the resolution of the FUV map to 13″ to match that of the H I map. In this map, the (median based) 1σ RMS scatter of the noise is about 2×10^{-6} mJy arcsec^{-2}.

We adopt inclination (24°) and position angle (225°) from Tilanus & Allen (1993), distance (D $\approx$ 4.5 Mpc) from Karachentsev et al. (2004) and the optical radius ($r_{25} \approx 7.7'$) from LEDA (Paturel et al. 2003). For details of data processing, the conversion of measured intensities to physical units (e.g., FUV intensities into estimated SFR surface densities), assessment of uncertainties, etc., we refer the reader to Bigiel et al. (2010).

3. LOCATION OF FUV RELATIVE TO HI

Figure 1 shows that H I (lower left panel) and UV emission (top panels) are detected far into the outer disk of M83 (the edge of the maps corresponds to $\sim 3.5\,r_{25}$). It also shows a remarkable spatial coincidence of major features found in the maps. Figure 2 shows this even more clearly: Plotted are (smoothed) H I contours of $0.2\,M_\odot$ pc^{-2} ($\sim 2.5\times10^{19}$ atoms cm^{-2}) on top of the GALEX FUV map. Almost every H I feature has a corresponding feature in the FUV map. Even very remote structures, such as the tip of the extended, western H I arm show FUV emission and thus signs of recent star formation activity. This close correspondence implies that the extended H I disk represents the reservoir from which the young stars emitting the FUV emission are forming (presumably with an intermediate stage of bound molecular gas). It also implies, quite surprisingly, that massive star formation proceeds – if at a low level – almost everywhere H I is observed.

Figure 3 quantifies the coincidence of H I and FUV[8]. The y-axis gives the fraction of the total FUV (gray) or H I (black) flux found in regions (i.e., along lines-of-sight) with H I surface densities lower than the value on the x-axis. For example, for an x-axis H I surface density of 2 $M_\odot$ pc^{-2}, we identify all area (i.e., lines-of-sight) in the maps with $\Sigma_{HI} < 2$ $M_\odot$ pc^{-2}. We then add up the H I (FUV) emission from this area and divide this H I (FUV) flux by the H I (FUV) flux of the entire map to get the fraction of flux found below the H I surface density of 2 $M_\odot$ pc^{-2}. For comparison, we also plot (dotted line) the fraction of area as a function of H I surface density (e.g., in the above example the fraction of the entire M83 H I map with $\Sigma_{HI} < 2$ $M_\odot$ pc^{-2}).

The key point in Figure 3 is that the FUV curve (gray) tracks the H I curve (black) much more closely than it follows the area curve (dotted). The area curve is the expected distribution for FUV emission if it were randomly distributed across the map. The fact that the H I and FUV curves are quite similar thus shows that rather than being randomly distributed, the distribution of FUV flux seems to follow that of the H I. Also, while most of the area in our map is covered by low column (or no) H I, the FUV comes mostly from lines-of-sight with relatively high Σ_{HI}. For example, 90% of the area has H I surface densities $< 2M_\odot$ pc^{-2}, while only $\sim$ 25% of the FUV flux comes from this area. This behavior is expected if FUV is spatially correlated with H I emission and implies that a substantial amount of H I (high surface densities) seems to be a necessary prerequisite to star formation.

[8] For this plot (and the following) we exclude regions near foreground stars and background galaxies identified from the GALEX pipeline source catalogs and from comparing UV and optical imaging

4. RADIAL TRENDS

Having seen that FUV and H I emission are remarkably coincident, we now ask how the *amount* of FUV emission compares to the mass of H I along a line-of-sight. The H I is concentrated into features (the arms and filaments in Figures 1 and 2) with a relatively low filling fraction, and we have just seen that FUV emission is largely coincident with these features. Our approach here is to look at the mean ratio of H I-to-FUV *along these features* as a function of radius, asking "Where there is H I, what is its average surface density and what is the associated average FUV intensity?". For this, we consider only emission from areas that have H I surface densities (in a smoothed 30″ resolution version of the H I map) $\gtrsim 0.5\,M_\odot$pc^{-2}.

Figure 4 shows the average H I and FUV intensities along these features. Differences are immediately apparent: the FUV profile (gray) decreases over many orders-of-magnitude from the inner parts into the outer disk before it levels off at about $1.7r_{25}$ (note that the FUV emission is not corrected for internal extinction, which is significant at small radii). The FUV emission at large radii is still detected with good sensitivity; the profile is always well above the gray dotted line, which shows the typical 5σ sensitivity. This supports the qualitative conclusion from Figure 2 that the extended H I structures in M83 seem to coincide with FUV emission, indicating recent SF activity out to largest radii. In contrast to the FUV profile, the H I surface density (black) shows only a moderate change with radius. The typical (azimuthally averaged) H I surface density is $\sim 2-4\,M_\odot$pc^{-2}.

Assuming FUV emission to arise mostly from young massive stars forming at a steady rate, we can convert the measured FUV intensities into star formation rate surface densities, Σ_{SFR} (using the same procedure as Bigiel et al. 2010). Then the ratio of the two profiles Σ_{HI}/Σ_{SFR} (which is proportional to Σ_{HI}/I_{FUV}) is the H I depletion time, the time it takes (present day) SF to deplete the current supply of H I. This quantity is shown as a function of radius in the right panel of Figure 4 (note that inside $\sim 0.5r_{25}$ we do not expect Σ_{HI}/I_{FUV} to trace the gas depletion time, as both H_2 and extinction become important).

The H I depletion time rises from the optical disk r_{25} out to $\sim 1.7r_{25}$ and then remains relatively constant across the far outer disk of M83 at about 100 Gyr, i.e., many Hubble times. This very long timescale has several implications. First, it is much longer than the ~ 2 Gyr depletion time of the *molecular* gas observed in the inner disks of galaxies (Bigiel et al. 2008; Leroy et al. 2008). Assuming bound, molecular clouds form stars with roughly the same efficiency in the inner and outer disk, this extremely long H I depletion time suggests that the process of building these molecular clouds is the bottleneck for forming stars at large radii. Combined with the rather low H I columns that dominate at large radii, the regulating and / or limiting factor for star formation in these environments may well be that of driving the H I to high enough densities to trigger the atomic-to-molecular phase transition and subsequent star formation.

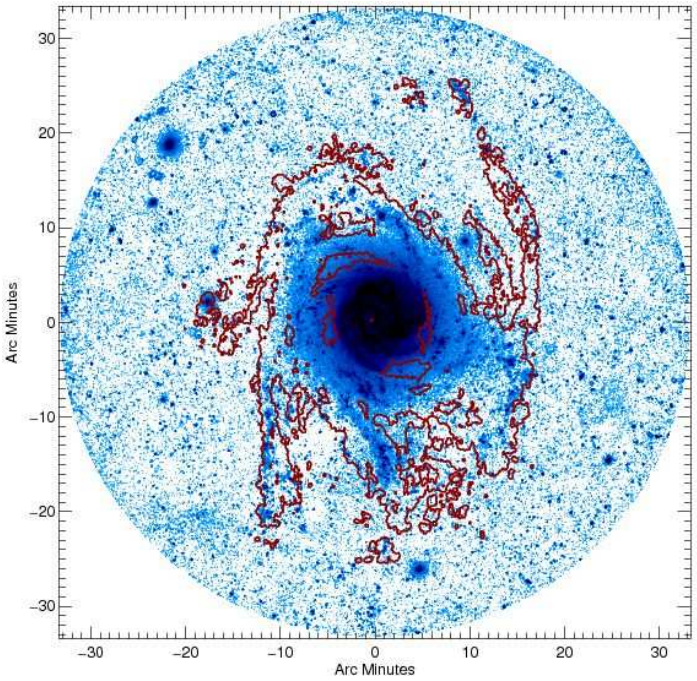

FIG. 2.— Smoothed HI contours of $0.2\,M_\odot$ pc^{-2} overplotted on the GALEX FUV map (compare Figure 1, upper left panel). The figure illustrates the close spatial correspondence of HI and FUV emission along the arms and filaments in the outer disk of M83.

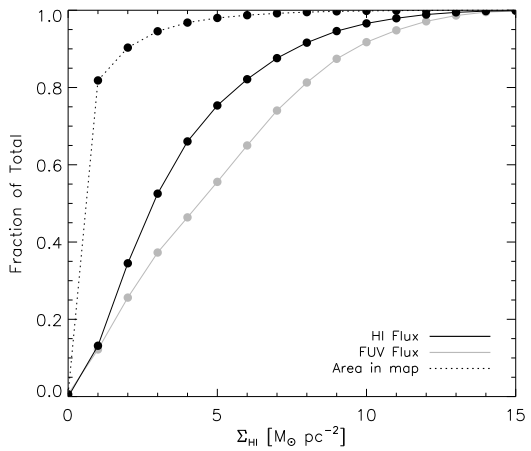

FIG. 3.— The distribution of FUV flux (gray), HI flux (black) and area (dotted line) in our maps as a function of HI surface density. The y-axis shows the fraction of the total HI or FUV flux or the fraction of area (relative to the entire map) below a given HI surface density (x-axis). Even though a large fraction of the M83 map is covered by little or no HI (dotted line), most of the FUV light comes from regions with relatively high HI surface densities (gray line).

The long H I depletion time also implies that the extended H I reservoir in the outer disk is long-lived, or at least that *in situ* star formation is unlikely to consume the gas. This means that this gas is in principle available as fuel for star formation in the inner disk, if it can be efficiently transported into the inner part of the galaxy (e.g., Wong et al. 2004; Vollmer & Leroy 2010). Single dish observations sensitive to the entire H I distribution (compare § 2) suggest that M83 hosts a very large reservoir of H I beyond the optical disk – as much as 80% of the total H I mass (Huchtmeier & Bohnenstengel 1981, and references therein). The total mass of this H I reservoir may well exceed $\sim 10^{10} M_\odot$, which would in principle be enough to sustain present-day SF in the inner disk of M83 for 2–3 times longer than is possible from the H_2 alone (Lundgren et al. 2004).

The moderate SF activity at large radii should also chemically enrich the H I envelope. If the disk remained in its present configuration for ~ 5 Gyr, then the integrated outer-disk SFR ($\sim 0.05\,M_\odot yr^{-1}$ beyond r_{25}) and a stellar yield of ~ 0.06 (Krumholz & Dekel 2010) imply a mass of heavy elements equal to about 1% of the total outer disk H I mass (as determined from our map). This is only a coarse estimate, but it shows that even the low observed outer disk SFR may enrich the outer disk gas to a moderate metallicity. This fits to observations of emission from hot dust (Dong et al. 2008) and fairly decent metallicities (Gil de Paz et al. 2007b; Bresolin et al. 2009) in the XUV disk of M83.

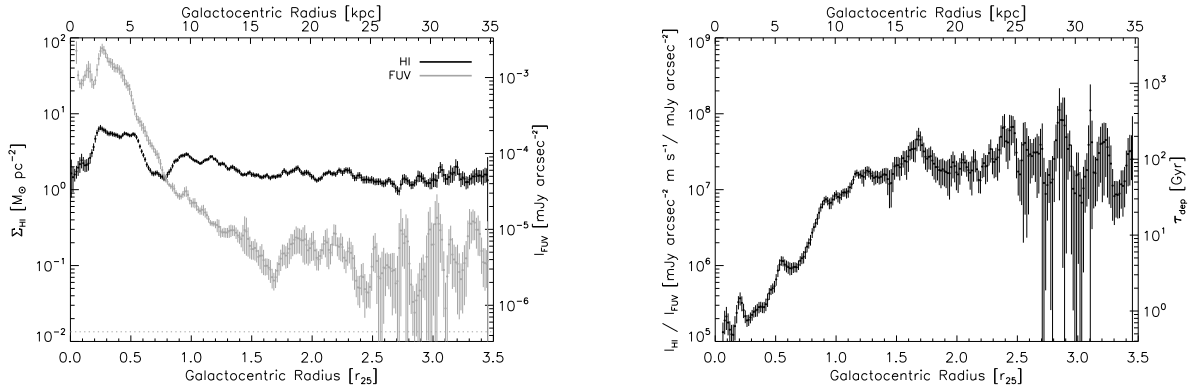

FIG. 4.— *Left:* HI (black) and FUV (gray) emission averaged in 6.5″ wide azimuthal rings (deprojected radial profiles) in regions of significant HI emission, i.e., along the arms in the extended disk of M83 (see text). The error bars show the (1σ) uncertainty in the mean in each annulus. The left axis provides the mass surface density scale for the HI profile, the right axis the intensity scale for the FUV profile (we note that in order to convert the FUV intensity scale – in units of mJy arcsec^{-2} – into SFR surface densities $\Sigma_{\rm SFR}$ – in units of $M_\odot yr^{-1}kpc^{-2}$ – one needs to multiply $I_{\rm FUV}$ by ~ 3.46; compare Bigiel et al. (2010)). The gray dotted line indicates the typical 5σ sensitivity for the (averaged) FUV emission in an (outer disk) annulus. The respective HI sensitivity is below the lower plot limit. HI and FUV emission show quite distinct radial trends: whereas average HI surface densities remain relatively constant along the filaments in the outer disk, the mean FUV intensity continues to drop before leveling off at $1.7r_{25}$. *Right:* Intensity ratio of HI and FUV radial profiles. Converting FUV intensity into $\Sigma_{\rm SFR}$, this ratio yields the HI depletion time (right axis). At large radii, this depletion time remains relatively constant at about 100 Gyr, i.e., many Hubble times.

5. DISTRIBUTION OF HI SURFACE DENSITIES

We have seen that low level star formation is pervasive in the H I arms and filaments in the outer disk of M83. We have also seen that the absolute level of this star formation is very low compared to that found in galaxy disks. What drives this drop in the fraction of H I that eventually ends up in stars? A number of authors have suggested that a drop in H I column or volume density leads to some critical prerequisite for cloud formation not being met (e.g., Elmegreen & Parravano 1994; Schaye 2004; Bush et al. 2010). We conclude by briefly examining how H I surface densities actually change between inner and outer disk.

The left panel in Figure 5 shows the (normalized) distribution of $\Sigma_{\rm HI}$ for lines-of-sight in different radial regimes (see caption for details). The right panel shows the same data, but now each line-of-sight is weighted by mass, so that the left panel gives the distribution of surface densities and the right panel shows at what column most of the mass is found.

In the left panel, the histograms from different regimes are not particulary distinct though one can see some enhancement in the H I columns found inside r_{25} (visible also as the "bump" in the radial profile in the left panel of Figure 4 between ~ 0.2 and $\sim 0.7\,r_{25}$). These differences are much easier to see in the mass-weighted histograms on the right. While in the optical disk H I surface densities between $\sim 2-8\,M_\odot$ pc^{-2} contribute roughly equally to the integrated H I mass in this regime, it is clearly the lowest H I columns that contribute most to the mass in the outer disk (i.e., beyond r_{25}). In fact, there appears to be a radial trend in the sense that as one moves inwards from the far outer disk, an increasing fraction of the H I mass comes from lines-of-sight with relatively high H I surface density.

We saw that in the outer disk of M83, high H I surface densities, likely a prerequisite for molecular gas and subsequent star formation, contribute a decreasing fraction to the overall H I mass as one moves to large radii. The extended arms seen in Figure 1 thus seem to represent merely the "tip of the iceberg" of the extended H I distribution in M83. These arms, however, appear to be the regions where pervasive star formation can proceed even at extreme galactocentric radii.

F.B. acknowledges support from NSF grant AST-0838258 and earlier support from the Deutsche Forschungsgemeinschaft (DFG) Priority Program 1177. Support for A.L. was provided by NASA through Hubble Fellowship grant HST-HF-51258.01-A awarded by the Space Telescope Science Institute, which is operated by the Association of Universities for Research in Astronomy, Inc., for NASA, under contract NAS 5-26555. We have made use of the NASA/IPAC Extragalactic Database (NED), which is operated by the Jet Propulsion Laboratory, California Institute of Technology, under contract with the National Aeronautics and Space Administration. This research has made use of NASA's Astrophysics Data System (ADS). We acknowledge the usage of the HyperLeda database (http://leda.univ-lyon1.fr).

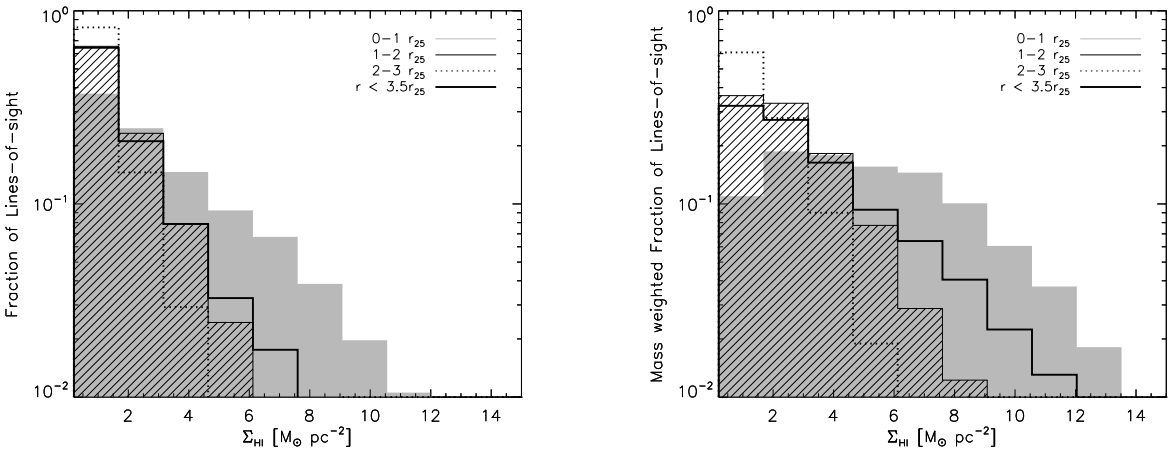

FIG. 5.— Normalized histograms of HI surface density (left panel) – the right panel shows the same distribution but mass-weighted – for each line-of-sight in 3 radial regimes: $0-1\,r_{25}$ (gray), $1-2\,r_{25}$ (black hashed), $2-3\,r_{25}$ (black dotted) and for the entire HI disk of M83 (thick black line). We bin emission between 0.2 (the sensitivity of the HI map) and $15\,M_\odot$ pc^{-2} in equally sized bins. The plots show that low HI columns dominate most of the area at all radii in M83 and that while higher columns contribute most to the mass within the optical disk, low column HI dominates the mass budget in the outer disk.

REFERENCES

Bajaja, E., Huchtmeier, W. K., & Klein, U. 1994, A&A, 285, 385
Bauermeister, A., Blitz, L., & Ma, C.-P. 2009, ApJ, accepted, arXiv:0909.3840
Bigiel, F., Leroy, A., Walter, F., Brinks, E., de Blok, W. J. G., Madore, B., & Thornley, M. D. 2008, AJ, 136, 2846
Bigiel, F., Leroy, A., Walter, F., Blitz, L., Brinks, E., de Blok, W. J. G., & Madore, B. 2010, arXiv:1007.3498, AJ, accepted
Blitz, L. in 25 Years of Millimeter Wave Spectroscopy, ed. W. B. Latter, S. J. E. Radford, P. R. Jewell, J. G. Mangum, & J. Bally (Dordrecht: Kluwer), 11
Boomsma, R., Oosterloo, T. A., Fraternali, F., van der Hulst, J. M., & Sancisi, R. 2008, A&A, 490, 555
Bosma, A. 1981, AJ, 86, 1791
Boissier, S., et al. 2007, ApJS, 173, 524
Braine, J., Ferguson, A. M. N., Bertoldi, F., & Wilson, C. D. 2007, ApJ, 669, L73
Bresolin, F., Ryan-Weber, E., Kennicutt, R. C., & Goddard, Q. 2009, ApJ, 695, 580
Bush, S. J., Cox, T. J., Hayward, C. C., Thilker, D., Hernquist, L., & Besla, G. 2010, ApJ, 713, 780
Cuillandre, J.-C., Lequeux, J., Allen, R. J., Mellier, Y., & Bertin, E. 2001, ApJ, 554, 190
de Blok, W. J. G., & Walter, F. 2003, MNRAS, 341, L39
Dong, H., Calzetti, D., Regan, M., Thilker, D., Bianchi, L., Meurer, G. R., & Walter, F. 2008, AJ, 136, 479
Elmegreen, B. G., & Parravano, A. 1994, ApJ, 435, L121
Ferguson, A. M. N., Wyse, R. F. G., Gallagher, J. S., & Hunter, D. A. 1998, ApJ, 506, L19
Gardan, E., Braine, J., Schuster, K. F., Brouillet, N., & Sievers, A. 2007, A&A, 473, 91
Gil de Paz, A., et al. 2005, ApJ, 627, L29
Gil de Paz, A., et al. 2007a, ApJS, 173, 185
Gil de Paz, A., et al. 2007b, ApJ, 661, 115
Huchtmeier, W. K., & Bohnenstengel, H.-D. 1981, A&A, 100, 72
Kamphuis, J., & Briggs, F. 1992, A&A, 253, 335
Karachentsev, I. D., Karachentseva, V. E., Huchtmeier, W. K., & Makarov, D. I. 2004, AJ, 127, 2031
Krumholz, M., & Dekel, A. 2010, in prep.
Lelièvre, M., & Roy, J.-R. 2000, AJ, 120, 1306
Leroy, A. K., Walter, F., Brinks, E., Bigiel, F., de Blok, W. J. G., Madore, B., & Thornley, M. D. 2008, AJ, 136, 2782
Lundgren, A. A., Wiklind, T., Olofsson, H., & Rydbeck, G. 2004, A&A, 413, 505
Martin, C. L., & Kennicutt, R. C., Jr. 2001, ApJ, 555, 301
Paturel, G., Theureau, G., Bottinelli, L., Gouguenheim, L., Coudreau-Durand, N., Hallet, N., & Petit, C. 2003, A&A, 412, 57
Pohlen, M., & Trujillo, I. 2006, A&A, 454, 759
Popescu, C. C., & Tuffs, R. J. 2003, A&A, 410, L21
Schaye, J. 2004, ApJ, 609, 667
Shlosman, I., Frank, J. & Begelman, M. C. 1989, Nature, 338, 45
Thilker, D. A., et al. 2005, ApJ, 619, L79
Thilker, D. A., et al. 2007, ApJS, 173, 538
Thilker, D. A., et al. 2009, Nature, 457, 990
Tilanus, R. P. J., & Allen, R. J. 1993, A&A, 274, 707
Vollmer, B., & Leroy, A. 2010, AJ, submitted
Walter, F., Brinks, E., de Blok, W. J. G., Bigiel, F., Kennicutt, R. C., Thornley, M. D., & Leroy, A. 2008, AJ, 136, 2563
Wong, T., Blitz, L., & Bosma, A. 2004, ApJ, 605, 183
Zaritsky, D. 1994, AJ, 108, 1619